Hindawi
International Journal of Antennas and Propagation
Volume 2019, Article ID 4601718, 10 pages
https://doi.org/10.1155/2019/4601718

Research Article

Design and Optimization of a Coherent Beamforming Network for an Aperiodic Concentric Ring Array

Armando Arce[1], **Enrique Stevens-Navarro**[2], **Marco Cardenas-Juarez**[2], **Ulises Pineda-Rico**[2], **Jorge Simon**[3] and **Marco A. Panduro**[4]

[1]*Catedras CONACYT and with Faculty of Sciences, Universidad Autonoma de San Luis Potosi (UASLP), 78290 San Luis Potosi, Mexico*
[2]*Faculty of Sciences, Universidad Autonoma de San Luis Potosi (UASLP), San Luis Potosi, Mexico*
[3]*Catedras CONACYT and Centro de Investigacion y Desarrollo en Telecomunicaciones Espaciales, Universidad Autonoma de Zacatecas (UAZ), 98000 Zacatecas, Mexico*
[4]*Department of Electronics and Telecommunications, CICESE Research Centre, 22860 Baja California, Mexico*

Correspondence should be addressed to Armando Arce; armando.arce@uaslp.mx

Received 18 December 2018; Accepted 12 February 2019; Published 6 May 2019

Academic Editor: Luciano Tarricone

In this work, a flexible and reconfigurable feeding network design for a nonuniform aperture on circular concentric ring arrays is proposed and analyzed. The network subsystem delivers coherent in-phase outputs with a Gaussian-like amplitude distribution, in a modular and basic topology based on sets of alternated power combiners and dividers. A complete antenna system in a monobeam configuration with a coherent network based on grouped inputs (blocks) per ring for an aperiodic concentric ring array with beam scanning and beam shaping properties is synthesized and analyzed. Additionally, a comparative analysis based on nonuniform and uniform concentric ring arrays fed by the proposed coherent network configuration is conducted and assessed. The optimization of the aperiodic layout on the antenna aperture (radii and interelement antenna spacings) is done by the differential evolution algorithm. Numeric experimentation demonstrates the performance advantages and capabilities of the proposed coherent network configuration with a nonuniform aperture over its uniform counterpart, with an improvement in average equal to −8.7 dB of side lobe level and 3.9 dB of directivity. Furthermore, the numeric examples show a complexity reduction on the coherent feeding network configuration based on the number of control signal inputs compared with a conventional phased antenna array; in the proposed configuration, the main beam is steered and shaped with N-1 control feeding ports per ring in this antenna system.

1. Introduction

Antenna arrays are an essential part of modern communication systems in various applications, offering an improved solution over single-element antennas. Thus, multiple antennas can radiate and synthesize contoured beams with advanced capabilities and features such as high-directive beams, electronic beam scanning (phased array), power pooling, among others.

Nowadays, there is a great interest in the development of advanced array systems where the focus is minimizing the total antenna system cost while maximizing the overall antenna system performance [1]. In this context, aperiodic arrays could improve the performance and in some cases could also reduce the number of antenna elements; however, their synthesis and optimization is a challenging task, where the additional degree of freedom is given by the layout that is employed to optimize the antenna array. This aperiodicity of the layout can also have meaningful additional complexity for the antenna system design and implementation if its corresponding feeding system is added.

An antenna system is not complete without its underlying feeding system, i.e., in every array, it can be discerned two main components: the first one are antenna elements, which are physically distributed over a specific area. The second is the beamforming network (BFN) subsystem; this

network is a crucial component for combining or feeding the antenna element's signal with the adequate amplitudes and phases to produce the desired beam [2, 3]. Traditional and well-known lossless beamforming networks are Blass [4], Butler [5], and Nolen [6] matrices. Despite their low-loss features advantages, these matrices tend to be more beam shaping restrictive due to the orthogonal excitation requisite and with less sophisticated beam scanning properties, diminishing the flexibility on the design [7]. Thus, a more recent alternative solution that improves reconfigurability and flexibility with electronic beam scanning and beam shaping capability is based on coherent networks. In recent years, a modular coherent network based on periodic structures called coherently radiating periodic structures has been presented [8]. This approach is based on an innovative design but with a minimalist topology just based on power dividers and combiners that deliver at the output an amplitude-tapered distribution with Gaussian shape. Thus, the coherently radiating periodic structures have been analyzed with different approaches over the years, in [9] as imaging systems to obtain high-resolution images, improving radiation features on arrays with patch-slot-patch (PSP) planar lens in [10] and in slot-coupled square patch antennas in [11]. As a beamforming network, the concept was introduced in [8, 12] with the methodology to design the feeding system for a linear array with the advantage of reducing the complexity to scan the beam. Some improvements on the efficiency were addressed in [13], and physical prototypes based on enhancements of the coherent network and its basic components were developed in [14, 15]. Moreover, the synthesis and optimization of the coherent beamforming network in different antenna geometries but with a periodic layout have been extensively addressed; related work can be found in [16–18]. Despite some initial investigations on aperiodic layouts with coherent networks in linear arrays have been revised in [19], the real potential of the network on aperiodic apertures has not been exploited.

This work presents an in-depth analysis of the performance of an antenna system that takes advantage from an aperiodic layout in circular concentric ring arrays with a simpler design of a coherent beamforming network with beam scanning capabilities. Hence, in this paper, a beamforming network design based on coherently radiating periodic structures to feed a nonequally spaced concentric ring array is proposed. Due to the optimization of the aperiodic aperture with the coherent network, both the radius and the interelement spacing on each ring are achieved by the differential evolution algorithm. To validate the effectiveness in performance of the proposed coherent network with the aperiodic antenna structure, a comparative analysis with the uniform layout with the same coherent network, in terms of side lobe level (SLL) and directivity (D), is performed and supported by numeric experimentation.

The remainder of this work is organized as follows: Section 2 addresses the aperiodic aperture formulation on circular concentric ring arrays, the theoretical model of a typical coherently radiating periodic structure as feeding network in a complete antenna system, and a description of the global optimization tool implemented. Section 3 presents the numeric experimentation setup for the coherent beamforming network configuration and its global optimizer, and in the same section, simulation and results for the antenna system are shown, analyzed, and discussed. Finally, in Section 4, conclusions of this work are presented.

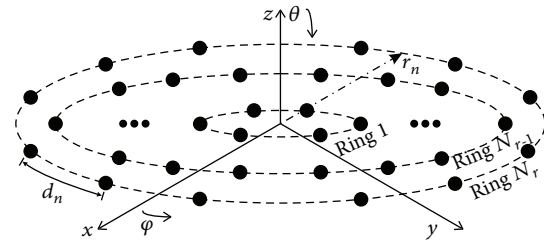

Figure 1: Typical geometry of a concentric circular ring array.

2. Problem Formulation

2.1. Aperiodic Concentric Ring Array. Let us consider a concentric ring array (CRA), i.e., multiple ring arrays with elements in a circular layout sharing a common center where each ring has its own radius. The concentric geometry assumes N_r rings and N_e antenna elements in each ring on the $x-y$ plane, as shown in Figure 1. The array factor considering point sources and an isophoric array feeding can be written as follows [20]:

$$AF(\theta,\varphi)=\sum_{n=1}^{N_r}\sum_{m=1}^{N_e}\exp[jk(x_{nm}(u)+y_{nm}(v))], \tag{1}$$

where $u-v$ space with its respective translation is given by $u=\sin\theta\ \cos\varphi-\sin\theta_0\ \cos\varphi_0$ and $v=\sin\theta\ \sin\varphi-\sin\theta_0\ \sin\varphi_0$ for a predefined direction of maximum radiation. Thus, the steering angle is denoted by (θ_0,φ_0) where the angles θ and φ are the spatial direction of radiation in elevation and azimuth, respectively.

Moreover, in (1), $k=2\pi/\lambda$ is the angular wavenumber, with λ representing the operating wavelength; $x_{nm}=r_n\cos\varphi_{nm}$ and $y_{nm}=r_n\sin\varphi_{nm}$ indicate the antenna element locations, where r_n represents the radial distance of each ring from the common center of the array until the nth ring, and the antenna element distribution around each circular ring (i.e., angular position) is denoted by $\varphi_{nm}=2\pi(m-1)/N_e$. Note that the array factor for the concentric array in (1) does not consider a central element in the origin.

Considering the aperiodicity in the concentric ring array [21–24], the array factor in function of the nonuniform interelement spacing in each ring d and the different radius of each ring r can be formulated as follows:

$$AF(\theta,\varphi,\boldsymbol{d},\boldsymbol{r})=\sum_{n=1}^{N_r}\sum_{m=1}^{N_e}\exp[jkr_n(u\cos\varphi_{nm}+v\sin\varphi_{nm})], \tag{2}$$

in which $\boldsymbol{d}=[d_{1,1},d_{1,2},\ldots,d_{1,N_1};d_{2,1},d_{2,2},\ldots,d_{2,N_2};d_{N_r,1},d_{N_r,2},\ldots,d_{N_r,N_p}]$, where d_{nm} denotes the arc longitude from

element m to element $m+1$ on the nth ring of the array; the radii of the antenna array are grouped in $\boldsymbol{r} = [r_1, r_2, \dots r_n]$ and $kr_n = 2\pi r_n/\lambda = \sum_{m=1}^{N_e} d_m, \forall n \in N_r$. An advantage of optimizing these variables (interelement spacings and ring radii) is a significative reduction of the dimensionality of the optimization problem that enhances the computational efficiency.

In this work, the optimization process for the beam pattern synthesis in the antenna system is accomplished by applying a global optimization technique. Thus, a global optimizer handles complex specifications and constraints in a heuristic cost function offering combinations of possible solutions to find a global near-optimal solution. The optimization problem is associated with an exponential function with a complex-valued argument (2) related to antenna element positions and the beam pattern, confronting a highly nonlineal and oscillating problem. Before the global optimizer's description, the mathematical expressions for the beamforming network considered as a part of the antenna system are described below.

2.2. Feeding Network Mathematical Model. A coherent network based on the principles of coherently radiating periodic structure beamforming network (C-BFN) is used in our numerical experiments. This network exploits the periodicity of a basic node, employed alternately as a power divider or combiner to propagate the signal until the antenna elements supported on the presence of a coherent coupling mechanism. The amplitude distribution at the output ports has a Gaussian shape and in-phase excitation law for each input port (true time delay) [14, 25]. In general, a feeding network topology can be implemented connecting and alternating basic nodes through successive layers, as shown in Figure 2. This particular diagram exhibits an example with the propagation of 3 different signals through the structure sharing the output ports. The power through the structure exhibits a binomial excitation law, where the coefficients are extracted from Pascal's triangle [8]. The versatility of the arrangement is the use of a basic node as a cornerstone, enabling to set different configurations with a varying number of layers, inputs, and outputs to design an antenna system with specific requirements. In this class of feeding networks, it is common to consider a greater number of output ports (N) than input ports (M) where the layers are determined by $N - M$.

The behavior of the basic node based on a 3-port component used for power division and combination is totally characterized by the following scattering matrix [8]:

$$[\boldsymbol{S}]_{\text{node}} = \begin{bmatrix} 0 & \frac{j}{\sqrt{2}} & \frac{j}{\sqrt{2}} \\ \frac{j}{\sqrt{2}} & 0 & 0 \\ \frac{j}{\sqrt{2}} & 0 & 0 \end{bmatrix}. \tag{3}$$

The ideal S-parameter matrix ensures no interaction between input signals assuming matching conditions at all ports. To assess the output of a C-BFN including the feeding network in an antenna synthesis problem, we can use a transfer matrix per layer $[\boldsymbol{T}_m]$ in a transmit mode given by the following expression [13]:

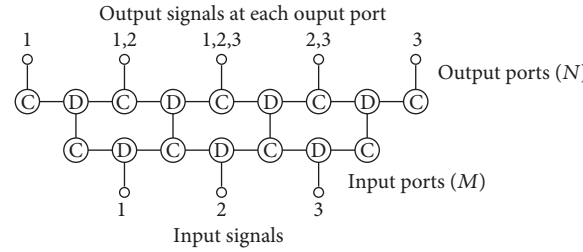

Figure 2: Diagram of a typical C-BFN topology based on basic nodes for power combination/division, which exemplifies the shared aperture for each input signal.

$$[\boldsymbol{\alpha}_{m+1}]_{(m+1,1)} = [\boldsymbol{T}_m]_{(m+1,m)} \cdot [\boldsymbol{\alpha}_m]_{(m,1)}, \tag{4}$$

in which $[\boldsymbol{\alpha}_{m+1}]$ denotes the output vector and $[\boldsymbol{\alpha}_m]$ is the input vector (complex excitation) at the feeding ports, both in the evaluated layer. The output vector is the resultant output of a C-BFN with one layer but it can be introduced as the input vector to design a C-BFN that involves more layers. In (4), m denotes the input ports and subscripts define the size of the matrices. Considering a C-BFN topology with more than one layer, with N output ports and M input ports, the behavior of the output excitation law $[\boldsymbol{\alpha}_N]$ of the feeding network can be found using (4) successively and is expressed as follows:

$$[\boldsymbol{\alpha}_N]_{(N,1)} = \left(\prod_{m=N-1}^{M} [\boldsymbol{T}_m] \right) \cdot [\boldsymbol{\alpha}_M]_{(M,1)}, \tag{5}$$

where $[\boldsymbol{T}_m]$ represents the transfer matrices of each layer in the feeding network and $m \in [N-1, N-2, \dots, M]$. The transfer matrices can be properly defined based on the transfer coefficients of the basic node in (3). A general transfer matrix of C-BFN can be formulated as follows:

$$[\boldsymbol{T}_m] = \frac{1}{2} \begin{bmatrix} \sqrt{2} & 0 & 0 & \cdots & 0 \\ 1 & 1 & 0 & \cdots & 0 \\ 0 & 1 & 1 & & \vdots \\ 0 & 0 & \ddots & \ddots & 0 \\ \vdots & \vdots & & 1 & 1 \\ 0 & 0 & \cdots & 0 & \sqrt{2} \end{bmatrix}_{(N,M)}. \tag{6}$$

From the matrix, it can be inferred that the columns denote power division and rows represent power combination. Thus, it is feasible to emulate and analyze a C-BFN, assembling a topology based on Figure 2 and assessing (4), (5), and (6). Thus, the coherent behavior of signals throughout the structure can be simulated in any numerical

computing environment or programming language. On the other hand, regarding C-BFNs, there is literature focused on its physical implementation that supports the above mathematical model. This practical research is based on replicating the basic constituting component by means of various multiport devices designed in microstrip technology, such as circular in-phase hybrid rings, Gysel power dividers/-combiners, or modified multiport Gysel devices [8, 14, 15]. In either case, it is necessary to ensure the in-phase behavior of a C-BFN, regardless of the antenna element periodicity (uniform or nonuniform). In some practical cases, an additional fixed phase shift to the branches is needed. The additional phase is typically introduced by adding an extra length, allowing that all outputs of each layer to be in-phase and the network operation can be predicted as in the mathematical model. Next, the global optimizer based on evolutionary computation used in this work is described.

2.3. Optimization Tool. Differential evolution (DE) is a well-known stochastic real parameter optimization tool used in this work to obtain a set of solutions for the antenna system. DE is a competent evolutionary algorithm widely used on electromagnetic problems including antenna design and beam pattern synthesis [26, 27]. The DE algorithm is used as an optimization tool for its proven efficiency on synthesis problems, a comparative analysis between this algorithm, and other population-based algorithms are out of the scope of this paper.

DE algorithm begins with a randomly initiated population (N_{pop}) constituted by real-valued vectors (in analogy with chromosomes) that enter in an iterative optimization cycle. These vectors form a candidate solution for a multidimensional problem. Thus, in the iterative process, some of these possible solutions are selected and geometrically perturbed with a scaled difference of two randomly chosen real-valued vectors in the population. The principal role on the optimization process is performed by the mutation operator, where for each real-valued and d-dimensional vector $\chi_i^G = [\chi_{i,1}^G, \chi_{i,2}^G, \dots, \chi_{i,d}^G]$ in the population at the G th generation (iteration), the mutated vector is expressed as follows:

$$\boldsymbol{v}_d^{G+1} = \chi_{r1}^G + F\left(\chi_{r2}^G - \chi_{r3}^G\right), \tag{7}$$

where the indices r_1, r_2, and r_3 are mutually exclusive integers randomly chosen from the total population. The parameter F denotes a positive control input for scaling the difference vectors $(\chi_{r2}^G - \chi_{r3}^G)$ which set the length of the exploration in the search space, known as mutation factor (typically with values between [0.4, 1]). Please refer to [28, 29] for a more detailed information of this population-based optimizer.

The optimization tool in this work is used to solve a constrained optimization problem to find a near-optimal solution of interelement spacing $\boldsymbol{d}$ for the nonuniform concentric ring array and the radius $\boldsymbol{r}$ of each ring in the concentric array, in order to achieve the lowest peak SLL and the maximum directivity in a predefined location of interest. This trade-off of antenna synthesis can be formulated as follows:

$$\begin{aligned} \min_{\boldsymbol{d},\boldsymbol{r}} \quad & \left\{\frac{|AF(\theta_{msl}, \varphi_{msl}, \boldsymbol{d}, \boldsymbol{r})|}{|AF(\theta_{\max}, \varphi_{\max}, \boldsymbol{d}, \boldsymbol{r})|}\right\} + \left\{\frac{1}{D(\theta, \varphi, \boldsymbol{d}, \boldsymbol{r})}\right\}, \\ \text{s.t.} \quad & |AF(\theta_{\max}, \varphi_{\max}, \boldsymbol{d}, \boldsymbol{r})| = 1, \\ & \boldsymbol{d} = \{d_n | \boldsymbol{d} \in \mathbb{D}\}, \quad \forall n \in N_e, \\ & \boldsymbol{r} = \{r_n | \boldsymbol{r} \in \mathbb{R}\}, \quad \forall n \in N_r, \end{aligned} \tag{8}$$

in which $(\theta_{msl}, \varphi_{msl})$ are the angles where the maximum side lobe is attained on either side of main lobe, $(\theta_{\max}, \varphi_{\max})$ indicate the main beam direction, $\mathbb{D}$ is the domain of interelement spacing in the antenna array, and $\mathbb{R}$ denotes the length of the radius domain of each ring.

The optimization process can be summarized as follows: DE algorithm randomly generates vectors (agents) as candidate solutions. These vector solutions of real numbers represent the variables to be optimized, in this specific case the element-to-element arc spacings for each ring $\boldsymbol{d} = [d_1, d_2, \dots d_n]$ and the radius of each ring $\boldsymbol{r} = [r_1, r_2, \dots r_n]$. Thus, each proposed solution vector suggests a radiation pattern to be evaluated that meets certain characteristics of side lobe level and directivity for a specific direction of interest in the antenna system. Afterward, the mutation process (7) in DE algorithm expands the search space, followed by the crossover operation which controls the number of components inherited from mutation operator with a predefined probability crossover rate (CR), promoting the diversity in population but affecting convergence speed. Later, the selection process secures the survival of the fittest solutions in subsequent generations and minimizes the possibility of population stagnation in the algorithm. Finally, DE obtains a global best solution that generates a radiation pattern with the design characteristics imposed, i.e., a radiation pattern with minimum side lobe level and maximum directivity in a predefined location in our experiments. The simulation setup and the numerical results to assess and validate the effectiveness of a C-BFN with an aperiodic concentric ring array (ACRA) are described in the next section.

3. Numeric Experimentation

In this work, the DE algorithm was implemented and employed to optimize the concentric ring array and the beamforming network. A random selection, one difference vector, and binomial crossover (DE/rand/1/bin) are the DE version applied for the optimization of the array factor. The DE algorithm is set up with an initial population of 120 individuals, with a mutation factor set in $F = 0.5$, a crossover rate $\text{CR} = 0.9$, and the maximum number of generations $G_{\max} = 1000$. The stochastic algorithm was executed for 20 independent trials for each direction of interest. The optimized array factor is a predominately function of the θ angle; the direction of maximum radiation can be found from a slice of the total array factor for a single value of φ (φ-cutting pattern).

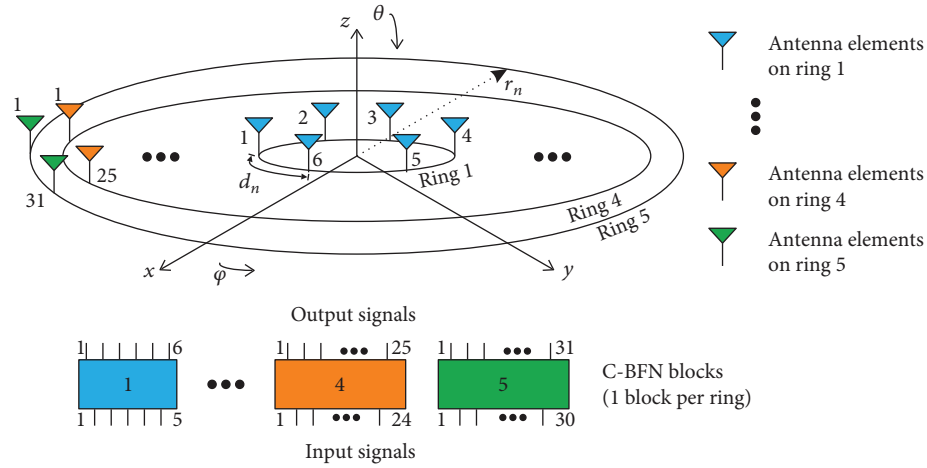

Figure 3: Schematic of the proposed feeding network configuration and its interconnection with the aperiodic concentric ring array.

The schematic of the system under study is shown in Figure 3, where an aperiodic concentric ring array is represented with nonequally spaced antenna elements and nonuniform spacing between rings. In our numerical experiments, in order to mitigate possible mutual coupling effects, the interelement spacing in each ring is at least $d_{\min} = 0.5\lambda$ and each ring is also set to be separated by a minimum distance of 0.5λ and $r_1 \geq 0.5\lambda$. Furthermore, without loss of generality, this schematic shows the concentric ring array composed by 92 antenna elements distributed in $N_r = 5$ rings, where the direction of interest is predefined at 45° for our numerical examples. The number of antenna elements on each ring is given by $N_e = 2\pi r_n / d_{\min} | r_n = n\lambda/2$, always taking the integer value, i.e., the antenna element distribution in each ring is $[N_1, N_2, N_3, N_4, N_5] = [6,12,18,25,31]$.

The coherent beamforming network is composed by Q blocks of 1 layer. The blocks integrate a complete C-BFN feeding network system, shown at the bottom of Figure 3. The proposed configuration to feed the nonuniform concentric array is formed by 5 C-BFN blocks; the number of blocks Q required per ring is equal to the number of rings N_r, i.e., one block for each ring in the antenna array. The indices at the ends of each block indicate the number of input signals (bottom part of each block) and the output signals (top of each block). The output ports (N) of each C-BFN block in this configuration are directly connected to an antenna element in each ring, as illustrated in Figure 3.

The objective for the specific proposed configuration is to assess the behavior of the beam radiation pattern conformed by a complete antenna system, i.e., the feeding network and the steerable aperiodic array. Furthermore, the purpose is to compare results with the same coherent network but with a uniform aperture (i.e., a uniform concentric ring array) to contrast performance. To test the possible improvements of a nonequally spaced over equally spaced concentric circular ring array in a coherent beamforming network with scanning capabilities, the worst solutions of an ACRA were compared with the uniform counterpart with the same proposed C-BFN configuration. The array factors generated are analyzed, and the complete antenna system is previously optimized by the evolutionary algorithm, under equal simulation settings and several trials. Thus, the aim in this numeric experimentation based on an optimization synthesis problem is to demonstrate and expose the performance advantages and complexity reduction of using a C-BFN on an aperiodic concentric ring array. In this context, three experimental cases were carried out based on the optimization variables where the main beam is generated with 87 input ports feeding all the aperture (92 antenna elements) for the uniform and nonuniform cases (see Figure 3). The experimental cases are described below.

3.1. Optimizing Antenna Rings ($\mathbf{r}$). The first variables optimized are the radii of the concentric ring array, with the goal of increasing the isolation level between the main beam and side lobes and favoring at the same time the antenna directivity. A comparative analysis of a C-BFN that feeds a concentric ring array was performed. In this numeric experimentation, the complete antenna system illustrated in Figure 3 was taken as a reference with the uniform and nonuniform spacing variants between rings for the concentric circular geometry. In this specific example, the antenna element spacings remain uniform in all rings with isophoric feeding (a unique excitation level).

Figure 4 illustrates the normalized power pattern for the monobeam configuration proposed (Figure 3) and described in detail at the beginning of this section (Section 3). In this numeric example, the main lobe is scanned along the azimuth plane and directed at 45° (predefined direction of interest). The specific type of geometry on the proposed antenna system and the optimization process applied to optimize the radius of each ring $\mathbf{r} = [r_1, r_2, \ldots, r_5]$ make possible to obtain a good performance in terms of side lobe level and directivity. The near-optimal ring spacings (radii) obtained by the algorithm in this first case were $[1.13\lambda, 1.74\lambda, 2.28\lambda, 2.86\lambda, 4.29\lambda]$, and the resulting aperture is arranged as shown in Figure 5(a).

The specific numerical values of SLL and D obtained and shown in Figure 4 are −14.49 dB and 15.35 dB, for a uniform concentric ring array (Uniform) with a C-BFN,

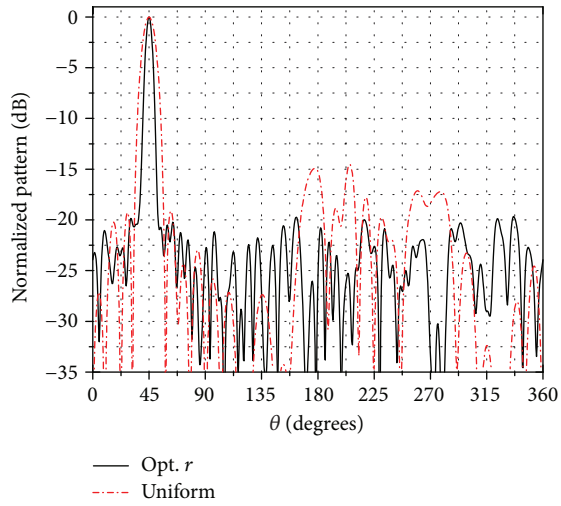

Figure 4: Comparison of normalized power patterns generated by the proposed C-BFN configuration with a uniform and nonuniform concentric ring array, optimizing r.

and -19.67 dB and 18.11 dB for the worst result of a C-BFN with a nonuniform spacing between rings (Opt. $\boldsymbol{r}$). Furthermore, in Figure 4, the general performance of the worst case of a normalized pattern in an ACRA with a C-BFN is better than the case of a radiation pattern in a uniform concentric ring array with the same beamforming network. The system behavior demonstrates that a coherent feeding network based on nonuniformly ring-spaced concentric ring array outperforms in equal conditions a uniformly ring-spaced concentric ring array fed by the same coherent network, in terms of side lobe level and directivity. The advantage in this specific example is equal to −5.18 dB of side lobe level and 2.76 dB of directivity; mean values are presented in Table 1.

3.2. Optimizing Antenna Elements ($\boldsymbol{d}$). In this numeric experiment, the variable optimized is the spacing between antenna elements of each ring on the concentric geometry. The optimization goal was the same established in (8), to reduce SLL and increase the antenna directivity. As in the numeric example above, the antenna system shown in Figure 3 was the proposed and considered beamforming network configuration that feeds the aperiodic concentric ring array, but now with the uniform and nonuniform interelement spacing variants for the concentric array. For this second experiment, an isophoric feeding with uniform spacings between rings is employed. The DE algorithm is used similarly to optimize antenna element spacings of all the rings $\boldsymbol{d} = [d_1, d_2, \dots, d_5]$. The element spacing solutions of the 5 rings given by the optimization algorithm were $[0.56\lambda, 0.62\lambda, 0.66\lambda, 0.85\lambda, 0.54\lambda]$, and the aperiodic layout is illustrated in Figure 5(b).

As in the above numeric example, Figure 6 shows the optimized power patterns generated by the antenna system under study (Figure 3) with uniform and nonuniform radiant elements. In this example case, the main beams were directed in a prefixed direction of interest, where the maximum radiation is set in 45°, as stated earlier.

Specifically, in Figure 6, the worst normalized pattern of a nonuniform interelement spacings plus the coherent beamforming network (Opt. $\boldsymbol{d}$) achieves -21.27 dB and 15.57 dB of SLL and D, respectively, in contrast to the uniform concentric ring array with the C-BFN (Uniform) shows specifically -14.49 dB and 15.35 dB. Moreover, as can be observed in Figure 6, the directivity for the predefined direction of interest on both cases for the ACRA and the uniform CRA fed by the coherent feeding network remains almost unchanged just with a minimal variation. In terms of side lobe level, the performance is clearly better for the nonuniform aperture with a C-BFN. In this numeric example, the gain is about -6.78 dB of isolation level (see Table 1).

3.3. Optimizing Antenna Elements and Rings ($\boldsymbol{d}, \boldsymbol{r}$). The last numeric optimization experiment involves the two variables of optimization previously analyzed at the same time, i.e., the ring and antenna interelement spacings of each ring, $\boldsymbol{r} = [r_1, r_2, \dots, r_5]$ and $\boldsymbol{d} = [d_1, d_2, \dots, d_5]$, respectively, on the concentric circular aperture. Once again, the proposed feeding network configuration and a concentric circular ring array (Figure 3) serve as a basis in this numeric experiment. A totally aperiodic antenna array (i.e., nonuniform interelement and ring spacings) is compared with its uniform counterpart, in terms of side lobe level and directivity, the trade-off of antenna parameters optimized and analyzed. For a predefined main beam direction ($\varphi = 45^\circ$) and considering only single level excitations (isophoric), the quasi-optimal solutions obtained by the global optimizer (DE) are $[0.54\lambda, 0.53\lambda, 0.56\lambda, 0.59\lambda, 0.55\lambda]$ for the antenna interelement distances and $[1.56\lambda, 2.26\lambda, 2.83\lambda, 3.57\lambda, 5.17\lambda]$ for the radii of all rings. The optimized geometry of the aperiodic antenna array is shown in Figure 5(c).

The resulting behavior of the normalized beam patterns generated by the proposed coherent beamforming network is shown in Figure 7. In this figure, the worst solution of the totally nonuniform concentric ring array with the proposed feeding network configuration (Opt. $\boldsymbol{d} + \boldsymbol{r}$) delivers -23.83 dB of side lobe level and 19.27 dB on the antenna directivity; in this case, as in the other numeric experiments, the uniform instance of the antenna system (Uniform) shows -14.49 dB and 15.35 dB, respectively, of the aforementioned antenna parameters.

Thus, Figure 7 clearly exhibits a better performance in the aperiodic circular ring array, in the antenna parameters under study (SLL and D), in comparison with the uniform concentric ring array fed by the same coherent network. The experiment shows dominance approximately about -8.31 dB of side lobe level and 3.82 dB of directivity; the result can be consulted and compared in Table 1. Furthermore, Figure 7 reveals a superior performance in SLL and D for the totally nonuniform antenna system (Opt. $\boldsymbol{d} + \boldsymbol{r}$) in contrast with the nonuniform interelement spacings (Opt. $\boldsymbol{d}$) and the nonequally spaced radii (Opt. $\boldsymbol{r}$) of the array on the proposed feeding network.

Numerical values of side lobe level and directivity for the antenna system with the proposed configuration of a coherent network for the uniform and nonuniform numeric

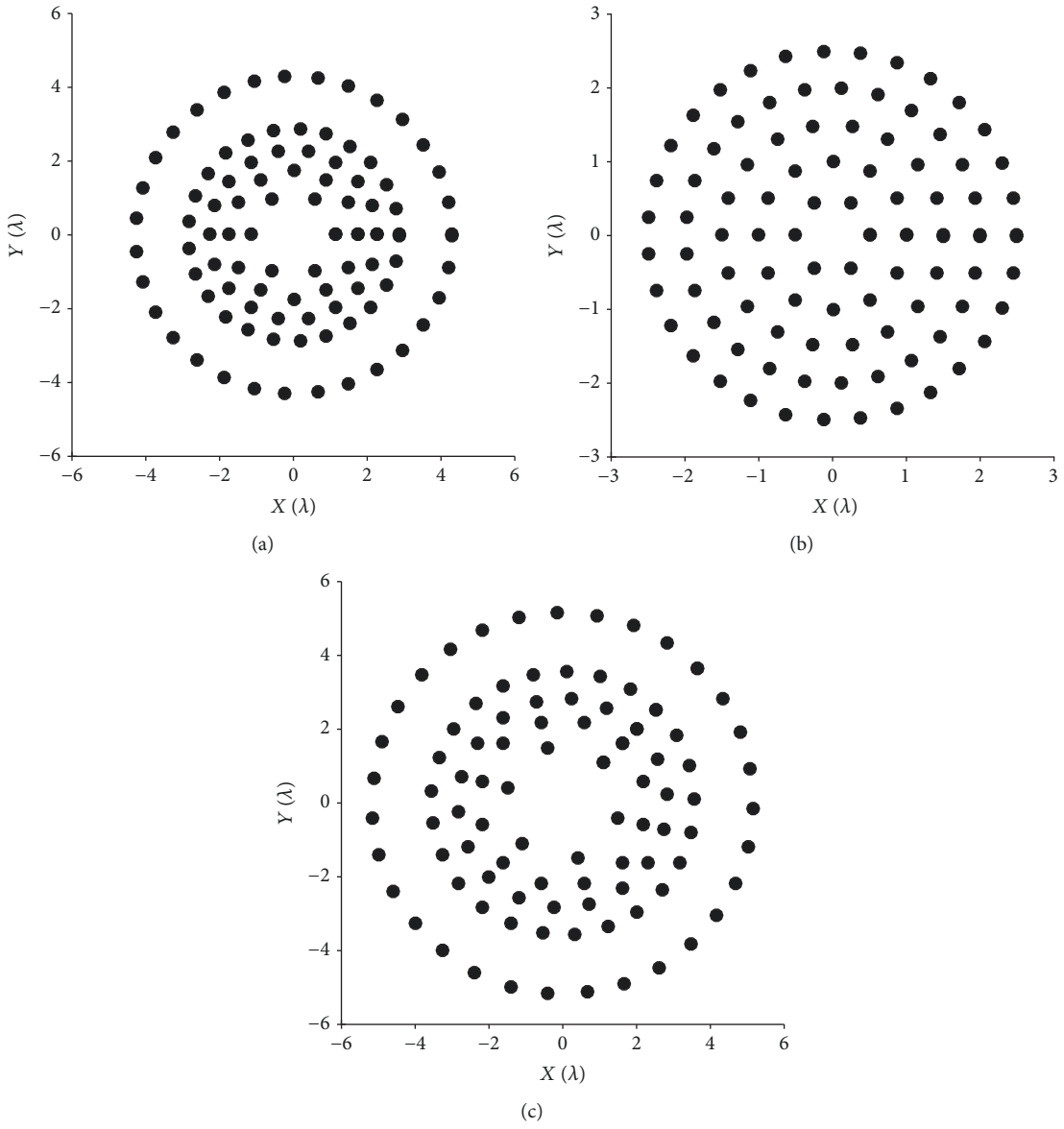

Figure 5: Aperiodic layouts of the concentric ring arrays in each numeric example: (a) optimizing antenna rings (r), (b) optimizing antenna elements (d), and (c) optimizing antenna elements and rings (d, r).

Table 1: Results of the numeric experiments presented and mean values of the nonuniformity improvement on the antenna system.

Antenna system (array + C-BFN)	SLL (dB)	D (dB)	ACRA + C-BFN improvement	
			SLL (dB)	D (dB)
Uniform	−14.49	15.35	—	—
Opt. r	−19.67	18.11	−5.7	2.6
Opt. d	−21.27	15.57	−6.8	0.1
Opt. $r + d$	−22.80	19.27	−8.7	3.9

examples are presented in Table 1. This table collects information on the worst numerical values of SLL and D obtained by the aperiodic concentric ring array with the coherent network for each numeric experiment (i.e., Opt. $\boldsymbol{r}$, Opt. $\boldsymbol{d}$, and Opt. $\boldsymbol{d} + \boldsymbol{r}$) and the values of the aforementioned parameters generated by the uniform concentric ring array (Uniform). Furthermore, Table 1 shows and groups the expected values of the improvement achieved by the aperiodic concentric ring array using the proposed feeding network for all the optimization experiments. In these experiments, the aperiodic aperture on each case is directly compared with the equivalent uniform aperture.

In general, a C-BFN that feeds a concentric ring array in uniform circular concentric geometry preserves basic behavior of circular arrays, with intrinsic high directivity but suffering from high side lobe levels throughout the steering range. Specifically, in the proposed coherent network configuration to feed an aperiodic concentric ring array based on subsets of inputs grouped by C-BFN blocks per ring, it maintains and reaches high numerical values of

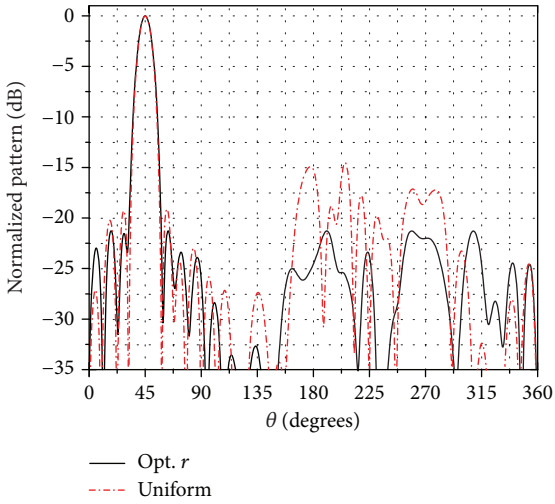

Figure 6: Comparison of normalized power patterns generated by the proposed C-BFN configuration with a uniform and nonuniform concentric ring array, optimizing d.

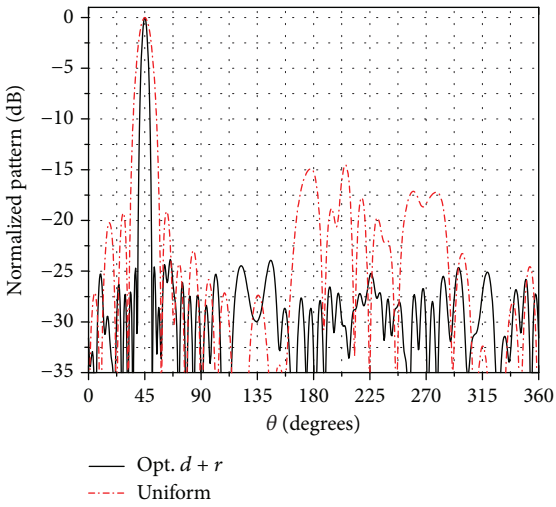

Figure 7: Comparison of normalized power patterns generated by the proposed C-BFN configuration with a uniform and nonuniform concentric ring array, optimizing d and r.

directivity (with an improvement between 2.6 and 3.9 dB on the mean) on fair and equal conditions on the optimization task. Nevertheless, in the specific numeric experiment that optimizes antenna elements (Opt. $\boldsymbol{d}$) in Table 1, the optimization algorithm cannot improve directivity meaningfully over the uniform CRA with the coherent network. On the other hand, all the nonuniform experiments (Opt. $\boldsymbol{r}$, $\boldsymbol{d}$, and $\boldsymbol{d}+\boldsymbol{r}$) with the proposed feeding network achieve high numerical values of side lobe level improving the uniform antenna system (Uniform), with a gain between -5.7 and -8.7 dB on average. Particularly, it is important to emphasize that the optimization of antenna elements and rings (Opt. $\boldsymbol{d}+\boldsymbol{r}$) at the same time on the antenna system clearly outperforms the optimization of a single variable in any nonuniform aperture.

From the comparative analysis related to circular concentric ring arrays shown in Figures 4, 6, and 7 and Table 1, the numeric experiments validate and ensure that the proposed coherent feeding network with an aperiodic concentric ring array has a better performance than a uniform concentric ring array with the same feeding network in terms of side lobe level and directivity. The optimized power patterns in this monobeam design demonstrate the capacity of the proposed antenna system to handle the trade-off between side lobe level and directivity in predefined directions of interest. Despite a prefixed direction of interest is defined in the numeric experimentation, the proposed C-BFN can conform and steer each beam to any direction under the window of visibility, with an isolation level and directivity that remain almost constant along the azimuthal plane, preserving basic properties of circular arrays, as stated earlier. For a fair analysis and to establish the maximum performance in terms of the antenna parameters under study (SLL and D), including an intrinsic complexity reduction of the network, the advantage of a sparseness optimization on the antenna array was avoided. Furthermore, in Figures 5(a) and 5(b), the optimized ring spacings (r) are assumed to be separated by a minimum distance of $\lambda/2$ with an additional separation ($0 \leq \Delta_\lambda \leq 1.5\lambda$) between rings. The resulting new optimized arrays exhibit a particular behavior where the first and last rings have the largest radius. This same behavior is also found in regular nonuniform concentric ring arrays where the element density in the radial direction is related to a low side lobe amplitude taper.

The proposed beamforming network design based on C-BFN for circular concentric ring arrays exploits its working principles to improve features over a conventional circular concentric aperture in a phased array with direct feeding, such as sharing paths coherently (coherent coupling) reducing control signal inputs. In the proposed design, the main beam is steered and shaped with N-1 input ports per ring, i.e., a reduction of one feeding port per ring without loss of antenna parameter performance. Although one way to increase the complexity reduction can be to add more layers to the beamforming design, a C-BFN of one layer topology was chosen in the proposed design to facilitate and ensure the in-phase behavior in a possible practical implementation. However, the proposed beamforming configuration is not unique on circular concentric ring arrays; different coherent network configurations can be proposed by varying or alternating input/output ports in the C-BFN blocks and incrementing the layers on the design. Due to the complexity reduction and shaping performance over all the steering range, the antenna system based on a C-BFN with an aperiodic circular concentric aperture is an alternative for various antenna applications.

4. Conclusion

A new design of a coherent beamforming network for an antenna system with an aperiodic circular concentric ring aperture, with shaping and steering capabilities, has been presented. The performance of normalized power patterns, which are conformed by the proposed beamforming network

configuration in a uniform and nonuniform concentric ring array, were compared and analyzed. The numeric experimentation shows that the proposed coherent network with isophoric feeding generates a main beam with shaping and steering properties, exploiting the aperiodicity of the antenna array with a reduced complexity of the antenna system. For the proposed feeding network configuration, which is based on subsets of feeding ports that are grouped by C-BFN blocks for each ring, numeric results show intrinsic high directivity values ($15.67 \leq D \leq 23.17$ on average) and significative low side lobe levels ($-20.19 \leq \text{SLL} \leq -23.20$ on average) with a reduction of the control signals inputs. The main beam is controlled and steered with N-1 feeding ports compared with a typical direct feeding system that needs one feeding port for each output port. A complete aperiodic concentric ring array improves its uniform counterpart in -8.7 and 3.9 dB on average of side lobe level and directivity, respectively. Future work is focused on the analysis of C-BFN for aperiodic concentric ring arrays in complex multibeam scenarios and in the full-wave electromagnetic simulation of the complete antenna system.

Data Availability

The numerical simulation data used to support the findings of this study are available from the corresponding author upon request.

Conflicts of Interest

The authors declare that there is no conflict of interests regarding the publication of this manuscript.

Acknowledgments

The research work presented in this paper has been supported by the Mexican Council of Science and Technology (CONACyT) under Grant no. 2016-01-1680 and the project Catedras (No. 872).

References

[1] H. E. A. Laue and W. P. du Plessis, "Numerical optimization of compressive array feed networks," *IEEE Transactions on Antennas and Propagation*, vol. 66, no. 7, pp. 3432–3440, 2018.

[2] J. Blake, E. Nygren, and G. Schennum, "Beamforming networks for spacecraft antennas," in *1984 Antennas and Propagation Society International Symposium*, pp. 158–161, Boston, MA, USA, USA, June 1984.

[3] P. Angeletti and M. Lisi, "Multimode beamforming networks for space applications," *IEEE Antennas and Propagation Magazine*, vol. 56, no. 1, pp. 62–78, 2014.

[4] J. Blass, "Multidirectional antenna - A new approach to stacked beams," in *1958 IRE International Convention Record*, vol. 8, pp. 48–50, New York, NY, USA, 1960.

[5] J. Butler, "Beam-forming matrix simplifies design of electronically scanned antennas," *Electronic Design*, vol. 12, pp. 170–173, 1961.

[6] J. Nolen, *Synthesis of Multiple Beam Networks for Arbitrary Illuminations, [Ph.D. dissertation]*, Radio Division, Bendix Corp., 1965.

[7] J. Allen, "A theoretical limitation on the formation of lossless multiple beams in linear arrays," *IRE Transactions on Antennas and Propagation*, vol. 9, no. 4, pp. 350–352, 1961.

[8] D. Betancourt and C. del Rio Bocio, "A novel methodology to feed phased array antennas," *IEEE Transactions on Antennas and Propagation*, vol. 55, no. 9, pp. 2489–2494, 2007.

[9] R. Garcia, D. Betancourt, A. Ibanez, and C. del Rio, "Coherently radiating periodic structures (CORPS): a step towards high resolution imaging systems?," *2005 IEEE Antennas and Propagation Society International Symposium*, vol. 4B, 2005, pp. 347–350, Washington, DC, USA, July 2005.

[10] D. Betancourt and C. del Rio, "PSP planar lens: a CORPS BFN to improve radiation features of arrays," in *2009 3rd European Conference on Antennas and Propagation*, pp. 1312–1315, Berlin, Germany, March 2009.

[11] A. Ibanez, R. Garcia, D. Betancourt, and C. del Rio, "Coherently radiating periodic structures (CORPS): a new perspective of designing antenna arrays," in *11th International Symposium on Antenna Technology and Applied Electromagnetics [ANTEM 2005]*, pp. 1–4, St. Malo, France, June 2005.

[12] D. Betancourt and C. del Rio, "3 by 3 phased array controlled by only three phase shifters," in *2006 First European Conference on Antennas and Propagation*, pp. 1–3, Nice, France, November 2006.

[13] N. Ferrando and N. J. G. Fonseca, "Investigations on the efficiency of array fed coherently radiating periodic structure beam forming networks," *IEEE Transactions on Antennas and Propagation*, vol. 59, no. 2, pp. 493–502, 2011.

[14] N. J. G. Fonseca, "Design and implementation of a closed cylindrical BFN-fed circular array antenna for multiple-beam coverage in azimuth," *IEEE Transactions on Antennas and Propagation*, vol. 60, no. 2, pp. 863–869, 2012.

[15] R. Zaker, A. Abdipour, and A. Tavakoli, "Full-wave simulation, design and implementation of a new combination of antenna array feed network integrated in low profile microstrip technology," *Analog Integrated Circuits and Signal Processing*, vol. 80, no. 3, pp. 507–517, 2014.

[16] M. A. Panduro and C. del Rio-Bocio, "Design of beam-forming networks using corps and evolutionary optimization," *AEU-International Journal of Electronics and Communications*, vol. 63, no. 5, pp. 353–365, 2009.

[17] A. Arce, D. H. Covarrubias, M. A. Panduro, and L. A. Garza, "A new multiple-beam forming network design approach for a planar antenna array using CORPS," *Journal of Electromagnetic Waves and Applications*, vol. 26, no. 2-3, pp. 294–306, 2012.

[18] A. Arce, M. Panduro, D. Covarrubias, and A. Mendez, "An approach for simplifying a multiple beam-forming network for concentric ring arrays using CORPS," *Journal of Electromagnetic Waves and Applications*, vol. 28, no. 4, pp. 430–441, 2014.

[19] A. Arce, M. Cardenas-Juarez, U. Pineda-Rico, D. H. Covarrubias, and E. Stevens-Navarro, "A multiple beamforming network for unequally spaced linear array based on CORPS," *International Journal of Antennas and Propagation*, vol. 2015, Article ID 757989, 7 pages, 2015.

[20] C. A. Balanis, *Antenna Theory: Analysis and Design*, John Wiley & Sons, New York, NY, USA, 3rd edition, 2005.

[21] R. L. Haupt, "Optimized element spacing for low sidelobe concentric ring arrays," *IEEE Transactions on Antennas and Propagation*, vol. 56, no. 1, pp. 266–268, 2008.

[22] L. Zhang, Y. C. Jiao, and B. Chen, "Optimization of concentric ring array geometry for 3D beam scanning," *International Journal of Antennas and Propagation*, vol. 2012, Article ID 625437, 5 pages, 2012.

[23] C. Bencivenni, M. V. Ivashina, and R. Maaskant, "Reconfigurable aperiodic array synthesis by compressive sensing," in *2016 10th European Conference on Antennas and Propagation (EuCAP)*, pp. 1–3, Davos, Switzerland, April 2016.

[24] A. A. Salas-Sanchez, J. Fondevila-Gomez, J. A. Rodriguez-Gonzalez, and F. J. Ares-Pena, "Parametric synthesis of well-scanning isophoric pencil beams," *IEEE Transactions on Antennas and Propagation*, vol. 65, no. 3, pp. 1422–1427, 2017.

[25] R. Rotman, M. Tur, and L. Yaron, "True time delay in phased arrays," *Proceedings of the IEEE*, vol. 104, no. 3, pp. 504–518, 2016.

[26] A. Deb, J. S. Roy, and B. Gupta, "A differential evolution performance comparison: comparing how various differential evolution algorithms perform in designing microstrip antennas and arrays," *IEEE Antennas and Propagation Magazine*, vol. 60, no. 1, pp. 51–61, 2018.

[27] S. Goudos, "Antenna design using binary differential evolution: application to discrete-valued design problems," *IEEE Antennas and Propagation Magazine*, vol. 59, no. 1, pp. 74–93, 2017.

[28] S. Das, S. S. Mullick, and P. N. Suganthan, "Recent advances in differential evolution - an updated survey," *Swarm and Evolutionary Computation*, vol. 27, pp. 1–30, 2016.

[29] P. Rocca, G. Oliveri, and A. Massa, "Differential evolution as applied to electromagnetics," *IEEE Antennas and Propagation Magazine*, vol. 53, no. 1, pp. 38–49, 2011.